

# Controllable coupling of superconducting flux qubits

S.H.W. van der Ploeg,<sup>1,\*</sup> A. Izmalkov,<sup>1</sup> Alec Maassen van den Brink,<sup>2,3,†</sup>  
U. Hübner,<sup>1</sup> M. Grajcar,<sup>4</sup> E. Il'ichev,<sup>1,‡</sup> H.-G. Meyer,<sup>1</sup> and A.M. Zagoskin<sup>3,5</sup>

<sup>1</sup>*Institute for Physical High Technology, P.O. Box 100239, D-07702 Jena, Germany*

<sup>2</sup>*D-Wave Systems Inc., 100-4401 Still Creek Drive, Burnaby, B.C., V5C 6G9 Canada*

<sup>3</sup>*Presently also at: Frontier Research System, RIKEN, Wako-shi, Saitama, 351-0198, Japan*

<sup>4</sup>*Department of Solid State Physics, Comenius University, SK-84248 Bratislava, Slovakia*

<sup>5</sup>*Physics and Astronomy Dept., The University of British Columbia,  
6224 Agricultural Rd., Vancouver, B.C., V6T 1Z1 Canada*

(Dated: October 26, 2019)

We have realized controllable coupling between two three-junction flux qubits by inserting an additional coupler loop between them, consisting of three Josephson junctions. Two of these are shared with the qubit loops and provide strong qubit-coupler interaction. The third junction gives the coupler a nontrivial current-flux relation; its derivative (i.e., the susceptibility) determines the coupling strength and sign, which thus are tunable *in situ* via the coupler's flux bias. In the quantum regime, in one sample we have achieved antiferromagnetic coupling with a strength  $J$  varying between  $\sim 44$  and  $\sim 85$  mK. In a second sample,  $J$  varied from  $\sim 45$  to  $\sim -55$  mK, where the latter indicates ferromagnetic coupling; in particular,  $J$  vanishes for an intermediate coupler bias.

PACS numbers: 85.25.Cp, 85.25.Dq, 03.67.Lx

The development of Josephson qubit devices has led to the realization of quantum gates [1–3] as well as two-[1, 4, 5] and four-qubit [6] coupling. For the implementation of real—say, adiabatic [7]—quantum algorithms, several hurdles must still be cleared: increasing the number of qubits and their coherence times is clearly desirable, but equally important is coupling tunability. In a number of promising proposals, the capacitances and inductances of classical circuit design are replaced with *effective* (“quantum”) capacitances [8] and inductances [9, 10], respectively, which are (sign-)tunable via their bias dependence.

Three-Josephson-junction (3JJ) flux qubits [11, 12] have a low sensitivity to charge noise, common to all flux-based designs. In addition, their small area protects them reasonably well against magnetic-flux noise, but limits the strength of their antiferromagnetic (AF) coupling via magnetic [5] or magnetic–kinetic [13] inductance. This can be overcome by using a *Josephson* mutual inductance [14], which can also be “twisted” for ferromagnetic (FM) coupling or (in theory) current-biased for limited tunability [15]. Recently, these and the above ideas were combined into a design involving a “quantum Josephson mutual inductance”, mediating a sign-tunable galvanic coupling between 3JJ qubits [16].

We report the first, to our knowledge, realization of *sign*-tunable coupling between solid-state qubits [17]. See Fig. 1: two 3JJ qubits  $a$  and  $b$  are connected to the coupler through shared junctions 7 and 9. The bias-line currents  $I_{b1,2}$  and the dc component  $I_{bT}$  of the tank current allow independent tuning of the three bias fluxes. The coupler's flux bias  $\Phi_c^x = f_c \Phi_0$  ( $\Phi_0$  is the flux quantum) tunes the phase difference across junction 8, and thus the interaction strength.

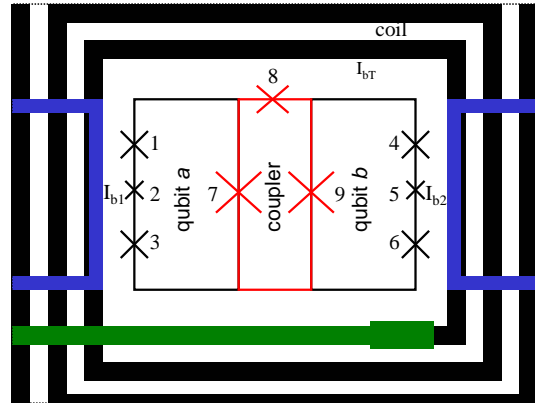


FIG. 1: Circuit design of sample 1. Junctions 123 form qubit  $a$ , junctions 456 form qubit  $b$ . The large qubit junctions have areas  $S_{1,3,4,6} = 150 \times 700 \text{ nm}^2$ , while  $\alpha_{a,b} = S_{2,5}/S_1 = 0.75$ . Junctions 789 form the coupler (in red), with areas  $S_{7,9} = 150 \times 2000 \text{ nm}^2$  and  $S_8 = 150 \times 1000 \text{ nm}^2$ . The ratio between the coupler and qubit loop areas is 2 : 3. The coil inductance is 135 nH, the tank-circuit capacitance is 470 pF ( $\omega_T/2\pi = 20.011 \text{ MHz}$ ,  $Q = 540$ ),  $M_{a,T} = M_{b,T} = 60.6$ ,  $M_{c,T} = 43$ ,  $M_{a,b1} = 1.5$ ,  $M_{b,b1} = 0.21$ ,  $M_{c,b1} = 0.43$ ,  $M_{a,b2} = 0.32$ ,  $M_{b,b2} = 1.8$ , and  $M_{c,b2} = 0.47$  (all in pH).

The system can be described by the effective pseudospin Hamiltonian [3, 5, 11, 12]

$$H = - \sum_{i=a,b} [\epsilon_i \sigma_z^{(i)} + \Delta_i \sigma_x^{(i)}] + J(\phi_c) \sigma_z^{(a)} \sigma_z^{(b)}, \quad (1)$$

where  $\epsilon_i$  is the bias on qubit  $i$ ,  $\Delta_i$  is the corresponding tunnelling matrix element,  $\sigma_z^{(i)}$ ,  $\sigma_x^{(i)}$  are Pauli matrices in the flux basis, and  $\phi_c \equiv 2\pi f_c$ .

To calculate the interaction strength  $J$  for a symmetric coupler  $E_{7,9} = E$ ,  $E_8 = \alpha_c E$ , consider the potential

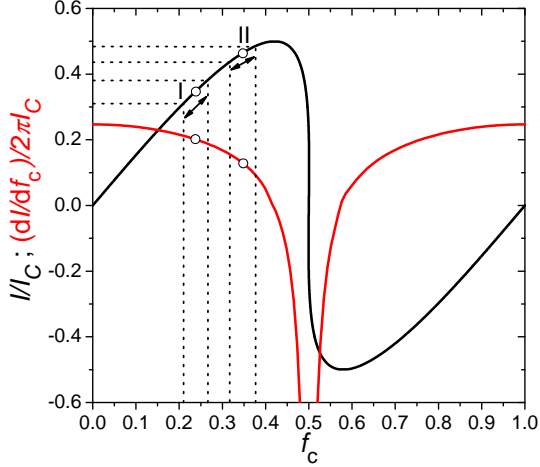


FIG. 2: The coupler's current–flux relation (black) and its derivative [red, see (4)], for a junction ratio  $\alpha_c = \frac{1}{2}$ . The coupler flux bias is  $f_c\Phi_0$ . I and II indicate the working points in Figs. 3 and 4, with function values 0.350 and 0.467, and slopes 0.203 and 0.127 respectively.

energy

$$U_J(\phi) = -E[\cos \phi_7 + \alpha_c \cos(\phi_c - \phi_7 - \phi_9) + \cos \phi_9] + U_a(\phi_a + \phi_7) + U_b(\phi_b + \phi_9), \quad (2)$$

where we implemented flux quantization for small-inductance loops, with  $\phi_{a,b}$  being the qubit flux biases in phase units, and where the qubit energies  $U_{a,b}$  are already minimized over their internal degrees of freedom  $\phi_{1-6}$ . However, each qubit has two minimum states, with opposite values of the persistent currents  $-(2e/\hbar)U'_{a,b} = \pm I_{pa,b}$ . We minimize  $U_J(\phi)$  with respect to  $\phi_{7,9}$ , and expand in  $E^{-1}$ . This implements the classical limit of the general condition that the coupler should stay in its ground state, following the qubits adiabatically [8]. To leading order, the phases obey  $\phi_7 = \phi_9 = \bar{\phi}$ , with  $\sin \bar{\phi} = \alpha_c \sin(\phi_c - 2\bar{\phi})$ . Proceeding to  $\mathcal{O}(E^{-1})$  and retaining terms  $\propto I_{pa}I_{pb}$ , one finds

$$J(\phi_c) = \frac{\hbar}{2e} \frac{I'(\phi_c)}{I_c^2 - I(\phi_c)^2} I_{pa}I_{pb}, \quad (3)$$

in terms of the coupler current  $I(\phi_c) = I_c \sin \bar{\phi}$  with  $I_c = (2e/\hbar)E$ , so that

$$I'(\phi_c) = I_c \frac{\cos(\bar{\phi})\alpha_c \cos(\phi_c - 2\bar{\phi})}{\cos(\bar{\phi}) + 2\alpha_c \cos(\phi_c - 2\bar{\phi})}. \quad (4)$$

Both  $I(\phi_c)$  and  $I'(\phi_c)$  are plotted in Fig. 2 for  $\alpha_c = 0.5$  as in Fig. 1. For  $\alpha_c \ll 1$ , one has  $I(\phi_c) \approx \alpha_c I_c \sin \phi_c$ , so that  $J(\phi_c) \approx (\hbar^2 \alpha_c \cos \phi_c / 4e^2 E) I_{pa}I_{pb}$ , the result from Ref. [16]. Hence,  $J(\phi_c) > 0$  ( $< 0$ ) near  $\phi_c = 0$  ( $\pi$ ), corresponding to AF (FM) coupling.

In our experiment,  $I_{pa,b}$  in fact are not negligible ( $\sim \frac{1}{4}I_c$ , see the caption to Fig. 1), and the separation of

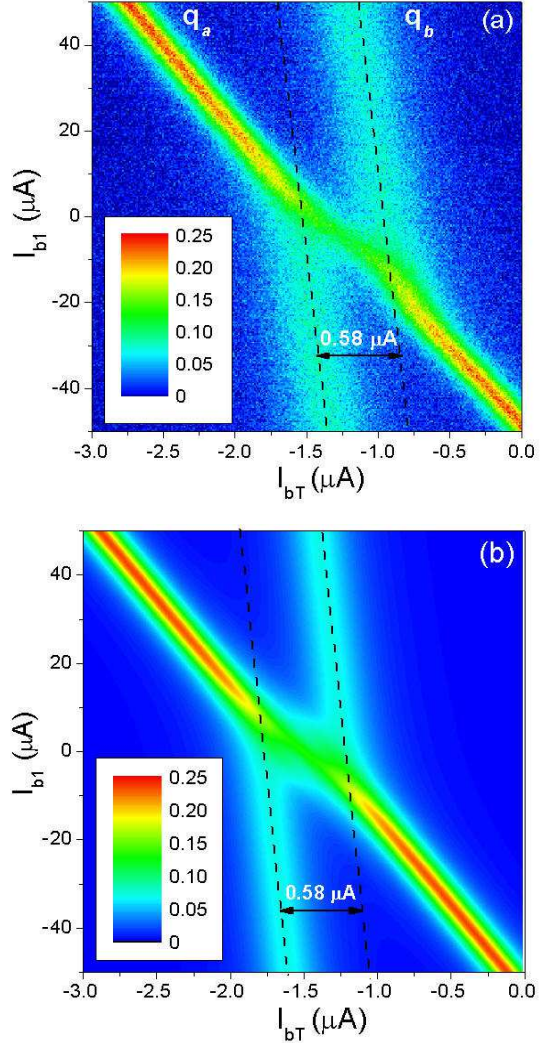


FIG. 3: (a) –  $\tan \theta(I_{bT}, I_{b1})$  for sample 1 at  $I_{b2} = 0$ . At the qubits' co-degeneracy point, the coupler flux equals  $0.237\Phi_0$  (point I in Fig. 2). (b) Theoretical fit to (1). A quick estimate for the coupling constant is  $J = \frac{1}{2}\Delta I_{bT}M_{b,T}I_{pb} \approx 85$  mK.

energy scales leading to distinct, well-defined, qubits and coupler in (1), (3) is incomplete (see also below Fig. 6). Still, the analysis holds qualitatively [18].

The qubit–coupler circuit was fabricated out of aluminum, and the pancake coil out of niobium [5, 6, 15]. Besides providing an overall dc field bias, the coil is part of a resonant  $LC$  tank circuit, operating well below the characteristic qubit frequencies. In the Impedance Measurement Technique [19], one records the current–voltage phase angle  $\theta$  in the tank, which is very sensitive to its effective inductance, and hence to the peaks in qubit susceptibility associated with level anticrossings [20].

Figures 3 and 4 present results for  $\tan \theta$  versus the bias currents  $I_{bT}$  and  $I_{b1}$ , for sample 1 with parameters as in Fig. 1. The conversion from current to flux biases can be calibrated using the flux periodicity (not shown),

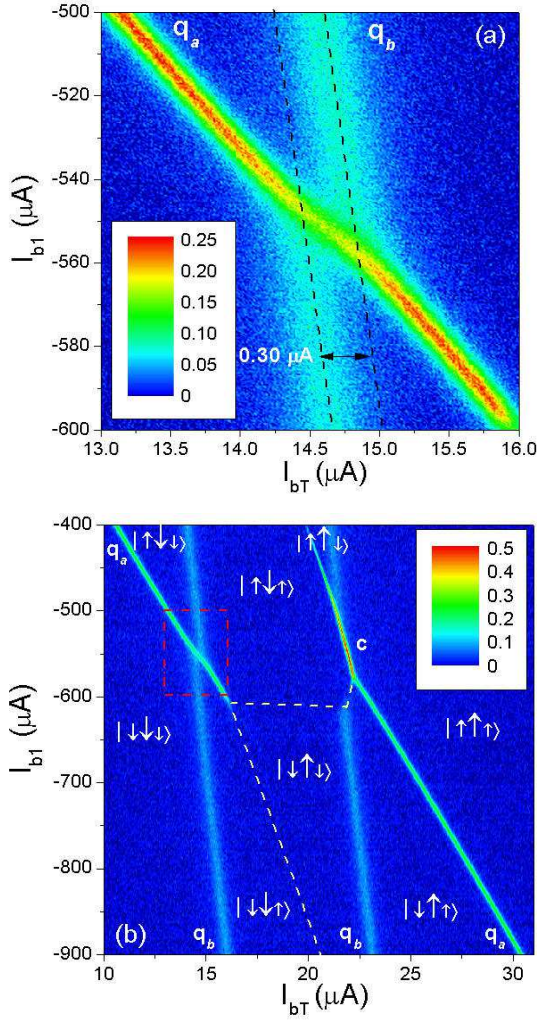


FIG. 4:  $-\tan \theta(I_{bT}, I_{b1})$  for sample 1 at  $I_{b2} = 450 \mu\text{A}$ . (a) Close-up of the co-degeneracy point [dashed box in (b)], where the coupler flux is  $0.347\Phi_0$  (point II in Fig. 2). (b) Overview and stability diagram. The sizes of the arrows denote the relative magnitudes of the loop currents in qubit  $a$ , coupler, and qubit  $b$  respectively.

and the system parameters as well as the effective temperature  $T$  can be extracted by fitting the data to the Hamiltonian (1), both as usual [5, 6, 15, 19].

In Fig. 3, the current through the second bias line  $I_{b2}$  is set to zero. The qubits are at co-degeneracy [ $\epsilon_a = \epsilon_b = 0$  in (1)] for a coupler flux  $f_c = 0.237$ . We find the persistent currents  $I_{pa} = 130 \text{ nA}$ ,  $I_{pb} = 70 \text{ nA}$ , tunneling amplitudes  $\Delta_a \approx \Delta_b \approx 70 \text{ mK}$ , as well as the coupling strength  $J \approx 85 \text{ mK}$  [see Fig. 3(b)]. The quantitative agreement between the theory based on (1) and the experimental data confirms that the system is in the quantum regime. In Fig. 4, a bias current  $I_{b2} = 450 \mu\text{A}$  is applied. As a result, the co-degeneracy point is shifted to  $f_c = 0.347$ . Compared with Fig. 3, the coupling strength is reduced to  $J = 85 \times (0.30/0.58) \approx 44 \text{ mK}$  [Fig. 4(a)].

The corresponding working points are marked in Fig. 2.

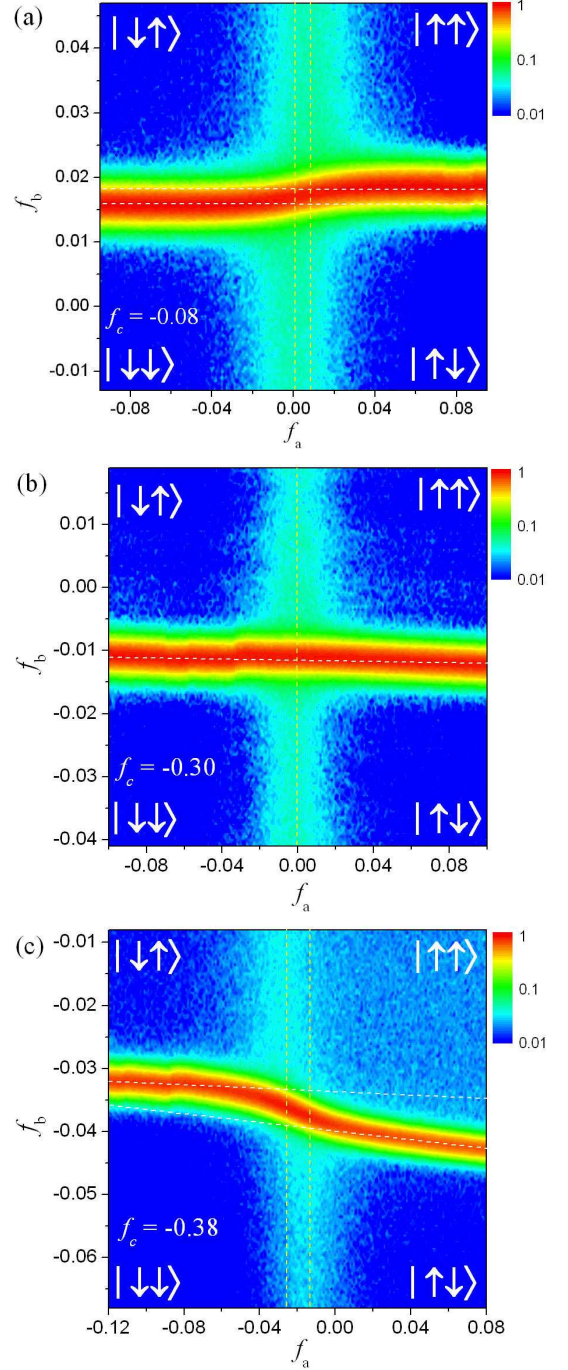


FIG. 5:  $-\tan \theta(f_a, f_b)$  for sample 2 at coupler bias  $f_c = -0.08$ ,  $-0.30$ , and  $-0.38$  respectively. A theory fit analogous to the one in Fig. 3(b) yields couplings  $J = 45$ ,  $0$ , and  $-55 \text{ mK}$ . The excess response in the  $|\uparrow\uparrow\rangle$  quadrant for  $f_c = -0.38$  is due to the coupler, cf. Fig. 4(b).

Since FM coupling should only occur for  $|f_c - \frac{1}{2}| \ll 1$ , the parameters of sample 1 allow varying the strength of AF coupling, but are not auspicious for switching its sign. In fact, the coupler, with a junction ratio  $\alpha_c = 0.5$ , is on the very boundary of the hysteretic regime [12]. Hence, for  $f_c \approx \frac{1}{2}$ , the coupler will have a very small energy

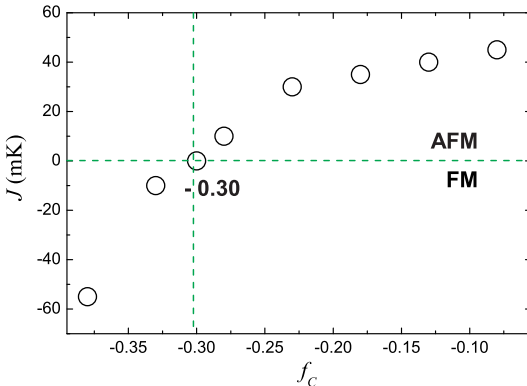


FIG. 6: The flux-tunable coupling strength  $J(f_c)$  for sample 2.

gap above its ground state and the adiabaticity condition mentioned above (3) breaks down, regardless of the exact value of  $\alpha_c - \frac{1}{2}$ . Indeed, in this case we rather observe *three*-qubit behaviour, with the coupler's own anti-crossing characterized by  $\Delta_c = 90$  mK and  $I_{pc} = 300$  nA [Fig. 4(b)]. This is fully consistent with our interpretation above, since the operating regimes are different.

Based on this experience, sample 2 was fabricated with a smaller junction 8 so as to have  $\alpha_c = 0.2$ . In addition, flux compensation (involving an additional wire  $I_{b3}$  preferentially biasing the coupler) facilitates independent tuning of the bias fluxes in the three loops. Results are shown in Fig. 5; one observes a progression from AF coupling, via virtually independent qubits, to FM coupling. This flux-bias dependence is shown in greater detail in Fig. 6. A fit yields the parameters as  $\Delta_a = 300$  mK,  $I_{pa} = 75$  nA,  $\Delta_b = 55$  mK, and  $I_{pb} = 180$  nA.

In conclusion, we have for the first time demonstrated sign-tunable Josephson coupling between two three-junction flux qubits, in the quantum regime. At  $T \approx 70$  mK, the coupling strength  $J$  was changed from +45 (antiferromagnetic) to -55 mK (ferromagnetic). At an intermediate coupler bias,  $J$  vanishes, thereby realizing the elusive superconducting switch. These results represent considerable progress towards adiabatic quantum computing in superconducting structures: control of  $J > 0$  is necessary to operate the computer, and ferromagnetic coupling ( $J < 0$ ) allows one to create dummy qubits, as used in the scalable architecture of Ref. [7]. While our measurements are essentially equilibrium, the design of Fig. 1 is also relevant in the ac domain, where the coupling is controlled by a resonant rf signal [21].

AMvdB thanks M.H.S. Amin and A.Yu. Smirnov for discussions, and the ITP (Chinese Univ. of Hong Kong) for its hospitality. AI, SvdP, and EI were supported by the EU through the RSFQubit and EuroSQIP projects, MG by Grants VEGA 1/2011/05 and APVT-51-016604 and the Alexander von Humboldt Foundation, and AZ by the NSERC Discovery Grants Program.

\* Electronic address: [simon.vanderploeg@ipht-jena.de](mailto:simon.vanderploeg@ipht-jena.de); SvdP and AI contributed equally to this work.

† Electronic address: [alec@riken.jp](mailto:alec@riken.jp)

‡ Electronic address: [evgeni.ilichev@ipht-jena.de](mailto:evgeni.ilichev@ipht-jena.de)

- [1] Yu.A. Pashkin, T. Yamamoto, O. Astafiev, Y. Nakamura, D.V. Averin, and J.S. Tsai, *Nature* **421**, 823 (2003).
- [2] T. Yamamoto, Yu.A. Pashkin, O. Astafiev, Y. Nakamura, and J.S. Tsai, *Nature* **425**, 941 (2003).
- [3] I. Chiorescu, P. Bertet, K. Semba, Y. Nakamura, C.J.P.M. Harmans, and J.E. Mooij, *Nature* **431**, 159 (2004).
- [4] A.J. Berkley *et al.*, *Science* **300**, 1548 (2003).
- [5] A. Izmalkov, M. Grajcar, E. Il'ichev, Th. Wagner, H.-G. Meyer, A.Yu. Smirnov, M.H.S. Amin, A. Maassen van den Brink, and A.M. Zagoskin, *Phys. Rev. Lett.* **93**, 037003 (2004).
- [6] M. Grajcar *et al.*, *Phys. Rev. Lett.* **96**, 047006 (2006).
- [7] W.M. Kaminsky, S. Lloyd, and T.P. Orlando, [quant-ph/0403090](https://arxiv.org/abs/quant-ph/0403090); M. Grajcar, A. Izmalkov, and E. Il'ichev, *Phys. Rev. B* **71**, 144501 (2005).
- [8] D.V. Averin and C. Bruder, *Phys. Rev. Lett.* **91**, 057003 (2003).
- [9] B.L.T. Plourde *et al.*, *Phys. Rev. B* **70**, 140501(R) (2004).
- [10] A. Maassen van den Brink, A.J. Berkley, and M. Yalowsky, *New J. Phys.* **7**, 230 (2005).
- [11] J.E. Mooij, T.P. Orlando, L. Levitov, L. Tian, C.H. van der Wal, and S. Lloyd, *Science* **285**, 1036 (1999).
- [12] T.P. Orlando, J.E. Mooij, L. Tian, C.H. van der Wal, L.S. Levitov, S. Lloyd, and J.J. Mazo, *Phys. Rev. B* **60**, 15398 (1999).
- [13] J.B. Majer, F.G. Paauw, A.C.J. ter Haar, C.J.P.M. Harmans, and J.E. Mooij, *Phys. Rev. Lett.* **94**, 090501 (2005).
- [14] L.S. Levitov, T.P. Orlando, J.B. Majer, and J.E. Mooij, [cond-mat/0108266](https://arxiv.org/abs/cond-mat/0108266); J.R. Butcher, graduation thesis (Delft University of Technology, 2002); for an application to charge-phase qubits, see J.Q. You, J.S. Tsai, and F. Nori, *Phys. Rev. B* **68**, 024510 (2003); for a related design featuring some tunability, see M.D. Kim and J. Hong, *Phys. Rev. B* **70**, 184525 (2004).
- [15] M. Grajcar *et al.*, *Phys. Rev. B* **72**, 020503(R) (2005).
- [16] A. Maassen van den Brink, [cond-mat/0605398](https://arxiv.org/abs/cond-mat/0605398).
- [17] See also R. Harris *et al.*, in preparation.
- [18] Estimating  $I_c \sim 4[\frac{1}{2}(I_{pa}+I_{pb})] \sim 400$  nA, from (3) one finds  $J \approx 125$  mK and 88 mK for points I and II respectively. As expected, ignoring quantum, thermal, etc. effects leads to an overestimation of  $J$ , which gets progressively worse as one approaches  $f_c = \frac{1}{2}$ , where, for sample 1, the whole analysis breaks down.
- [19] E. Il'ichev *et al.*, *Fiz. Nizk. Temp.* **30**, 823 (2004).
- [20] Ya.S. Greenberg, A. Izmalkov, M. Grajcar, E. Il'ichev, W. Krech, H.-G. Meyer, M.H.S. Amin, and A. Maassen van den Brink, *Phys. Rev. B* **66**, 214525 (2002).
- [21] M. Grajcar, Y.-X. Liu, F. Nori, and A.M. Zagoskin, [cond-mat/0605484](https://arxiv.org/abs/cond-mat/0605484).